Turkish Journal of Engineering
https://dergipark.org.tr/en/pub/tuje
e-ISSN 2587-1366

Analysis of explosion images obtained with high-speed camera with image processing and prediction of explosion loads

Dilan Onat Alakuş*[1], İbrahim Türkoğlu [2]

[1]*Kirklareli University, Software Engineering, Kırklareli, Turkey, onatalakus.dilan@klu.edu.tr*
[2]*Firat University, Faculty of Technology, Software Engineering, Elazığ, Turkey, iturkoglu@firat.edu.tr*

Cite this study: Onat Alakuş, D., & Türkoğlu, İ. (2025). Analysis of explosion images obtained with high-speed camera with image processing and prediction of explosion loads. Turkish Journal of Engineering. 9(3), 479-489

https://doi.org/10.31127/tuje.1524358

Keywords
Blast waves
Image processing
Blast loads
Prediction

Research/Review Article
DOI:
Received:
Revised:
Accepted:
Published:

Abstract

Visual data-based analysis of explosion events is important in areas including security, disaster management and industrial safety. Understanding the distribution of these events not only helps detect them as they happen, but also facilitates informed decision making for mitigation and intervention strategies. Various experimental methods have been used in the literature on this subject and empirical formulas have been produced. These formulas are still used today, but they are based on limited experimental data. Statistical methods measure the distribution of these data, allowing measurements such as frequency and spatial clustering to identify patterns in the analyzes obtained from the experimental data. Visualization tools further explain these findings, helping to understand and support decision. During and after the explosion, various effects arise from the explosion. These effects are effects such as sound, explosion-induced flash of light, blast wave, craters, tremors. Various sensors are used to measure these effects. These sensors can be damaged during explosion or when used for experimental methods and are very costly. The aim of the study is to increase the predictability of security measures and to reduce the need for high-cost devices by using classical image processing methods. Explosion images were obtained using a high-speed camera for this study. The aim of the study is to analyze blast waves, which are the most fundamental and most destructive effect of the explosion event. Explosion waves occur at a speed imperceptible to the human eye and are damped in very short periods of time. These waves were tried to be detected by using a high-speed camera and image processing methods, and it was aimed to obtain information about explosive charges from these waves. As a result of the study, blast waves have been successfully detected and explosive loads have been successfully analyzed using experimental studies in the literature.

1. Introduction

Explosions can occur in various ways, controlled or uncontrolled, due to natural disasters, terrorist attacks, security vulnerabilities or experimentally [1]. Detecting explosions before they occur or fully analyzing their effects after they occur is of critical importance to reduce the negative effects of such events and provide rapid intervention. Explosion is basically an event that suddenly spreads in the air environment with high heat, high sound and high energy, which occurs when three sources: ignition source, oxygen and explosive material come together, and is damped when the pressure equalizes the pressure in the air environment [2]. It can be fatal due to the high temperature and high pressure it contains. Explosion basically occurs in two different ways including controlled. and uncontrolled explosions. Controlled explosions are carried out under expert control. Explosions occur in two distinct ways, including controlled and uncontrolled. Controlled explosions, which are carried out under expert control, serve various purposes, such as building destruction, mine exploration, road construction, and scientific studies [3]. On the other hand, uncontrolled explosions occur spontaneously and without precautions, including terrorist attacks, gas compression, and ammunition explosions [4].

Being able to analyze the effects of an explosion event is important in many respects. At the same time, it is very important to know the effects of a possible explosion before it occurs. Many experimental studies have been conducted in the past to analyze these effects. As a result of the experimental studies, many empirical formulas

and explosion data were obtained. All studies in the literature and the methods obtained from these studies have some limitations. For instance, the area where the explosion occurs and the resulting blast wave form, the amount of the explosive and the distance to the explosive location are some of these. In addition, determining blast loads and analyzing their possible effects is time-consuming because it is based on empirical formulas.

Various methods are used to detect the distribution of blast waves, including image analysis, machine learning and artificial intelligence, integration of sensor data and statistical methods. Furthermore, the effects of an explosion are directly related to the type and amount of explosive. It is also related to the location of the explosive and the form the blast wave takes. After the explosion, many loads called blast loads occur. Blast load parameters are essential for information about the explosive and for analyzing the explosion effects. These loads are calculated using different methods depending on the explosive's location, type, and shape. Explosion occurs in three different ways depending on the location of the explosive. These are free air explosions, air explosions and surface explosions. In free air explosions, the explosive is detonated on the air and hits the structure before reaching the surface [5]. The explosion wave is outward and spherical. In air explosions, the explosive is detonated in the air and reaches the structure after hitting the ground [5]. After hitting the ground, a Mach wave is formed. The blast wave is outward and spherical, as in a free air explosion. Surface explosions are detonated on the ground or at very close distances to the ground. The explosion wave propagates hemispherically and outwards [5].

With today's technologies, these explosions are made in a controlled manner and explosion data are obtained from these experimental explosions. While these explosions are carried out, the amount of explosive and the type of explosive are determined in advance. However, in the event of a possible explosion or uncontrolled explosion, the amount of explosives is unknown, and their damage can only be determined after the explosion occurs. In addition, the damages of possible terrorist attacks in city planning and various structures and security applications cannot be known without an explosion. For these reasons, it is aimed to use image processing methods to detect the number of explosives and to provide solutions to the mentioned problems.

Researchers in the study [6] modelled the three-dimensional blast wave using background Schlieren imaging. The researchers prepared an experimental setup by using four cameras. Then, the background images were analyzed using Schlieren imaging. After the analysis process, edge extraction operations were performed on the images, and the waveform of an explosion was predicted. Study [7] describes an experiment of the background-oriented schlieren method (BOS) for quantitative visualization of open-air explosions. This method allowed quantitative visualization of the propagation curve of shock waves and the diffraction angle behind the shock waves. The results obtained using high-speed camera recordings and numerical analysis were compared. The results presented in the paper show that the BOS method can provide quantitative and conventional visualization results for outdoor experiments, and that better results can be achieved with the increased spatial resolution of high-speed cameras. Moreover, the obtained results show that the predicted overpressure distribution during the passage of shock waves is consistent with the values recorded by the pressure transducers at the test site. Experimental studies were carried out in study [8]. Experiments were performed using an open-ended shock tube, and a Canny edge detection algorithm was used to track the instantaneous positions of the shock waves. Additionally, information is given about a software system developed for more efficient and accurate processing of high-speed schlieren and shadowgraph images. This software system is developed based on MATLAB GUI and image processing toolbox [9]. The methods presented in the article can be used for visualization and analysis of high-speed flows. It has been stated that the developed software system and the methods used are an effective tool for the visualization and analysis of high-speed flows. In the experiments, it has been shown that the methods used to process schlieren and shadowgraph images are useful for tracking and analyzing the instantaneous positions of shock waves. Additionally, it has been stated that thanks to the developed software system, large data sets can be processed more efficiently and accurately. In conclusion, it is concluded that this study provides an effective method and tool that can be used for the visualization and analysis of high-speed flows. There are very few studies in this field in the literature. For this reason, the studies are limited. However, as seen in the studies reviewed, image processing is used as an effective method in determining shock waves. In this study, shock waves were analyzed with image processing and, unlike other studies in the literature, blast loads were also predicted.

This study aims to detect the blast wave from the images obtained from the explosion events carried out in a controlled manner, using image processing methods, and after detecting the blast wave on the image, it is aimed to determine the explosive weight, shock front velocity, blast wave pressure and positive phase durations. Explosion data were obtained from the Kingery-Bulmash polynomial formula, one of the empirical methods. Explosion images were obtained by controlling the detonating TNG (Trinitroglycerin) explosives of different weights. A high-speed camera was placed at a certain distance from the explosion area, and the moment of the explosion was recorded. These recorded images are then divided into frames. The resulting millisecond image frames were processed using image processing methods to obtain a blast wave from these images. Then, the aim was to predict the blast load parameters from the explosion waves obtained. The highlights of the study can be summarized as follows:

- Since experimental explosions are very few, there is not enough study in this field in the literature. Therefore, this study will contribute to the literature.
- When the studies were examined, only the explosion wave was analyzed using image processing methods. In this study, the

explosion wave was analyzed, and the blast loads were also predicted.

- In uncontrolled explosions, predicting blast loads with traditional approaches is time-consuming. However, with the method in this study, these loads could be predicted from a single image.

The remainder of the study is organized as follows. In the second section, a limited number of studies in this field in the literature are mentioned. In the third section, the data used in the study and the stages of obtaining these data are mentioned. In addition to these, the image processing techniques used are also highlighted in this section. In the fourth section, the application is emphasized, and the results obtained are supported with various images. In addition, a discussion was made in this section and the advantages and disadvantages of the study were explained. In the last section of the study, the study is summarized and the contribution of this study to the literature is mentioned.

2. Related Works

In addition to image processing, explosion images can also be analyzed using artificial intelligence and machine learning methods.

Researchers in the study [10], researchers utilized deep learning to predict pressure wave parameters in their study. Initially, a simulation environment was created to conduct an analysis of explosive effects. Through this simulation, accurate predictions were made for the intense pressure waves following an explosion, and their impacts on both individuals and structures were assessed. Additionally, a Deep Neural Network (DNN) was employed to identify overpressure data resulting from the explosions, specifically predicting pressures within the range of 1 to 5 meters. The classifier's performance was evaluated using Mean Square Error (MSE), resulting in a concluding Mean Square Error value of 20.84 for the Deep Neural Network model. In a separate investigation, scientists developed an early warning system by designing a deep learning model based on shock wave diagrams. Researchers in the study [11] commenced by converting a shock wave diagram into digital representations using a solver. Subsequently, edge extraction was executed, and Convolutional Neural Network (CNN) architecture was employed to detect the edges. The final step involved utilizing the Rectified Linear Unit (ReLU) activation function to extract crucial information pertinent to the study's objectives. This approach facilitated the acquisition of features for subsequent classification. In the classification phase, Long/Short Term Memory (LSTM) and Support Vector Machine (SVM) were applied as classifiers. The performance of each classifier was assessed and compared using accuracy as the evaluation criterion. At the conclusion of the study, the LSTM model exhibited a prediction accuracy of 92%, whereas this rate declined to 72% with the SVM model. Researchers in the study [12], investigators assessed the impact of explosions in an urban setting through simulation. The initial phase involved the utilization of aerial images, which were categorized through a semantic segmentation process. Subsequently, a 3D model was generated, incorporating the designed geometric structure. The study involved simulating explosions with weights of 1, 10, 100, and 1,000 kg. Throughout the prediction process, the analysis focused on the extent of damage to windows and glass breakage. The study concluded that, based on the simulation program, 1 kg of explosives could result in the breakage of 46 windows, 10 kg in 105 windows, 100 kg in 319 windows, and 1,000 kg in 363 windows. Researchers in the study [13], the researchers examine the injury potential and effects of shock waves, which are responsible for the primary effect. This study was carried out by creating two separate controlled explosions of varying power and capturing the moments of the explosions with the help of a high-speed camera, and then analyzing and using these images after recording. A fast camera recording 9,000 frames per second was used to record the images. In the first test, 100 g of TNT was detonated under a 70 kg display mannequin filled with gel. In the second test, 1000 g of C4 was placed at a height of 30 cm above the ground to simulate a bomb trap explosion in an open area. Mannequins placed around these blast sites were also used to observe the blast effects. The explosions were carried out with an electric detonator and the images were captured by placing a Photron Fastcam-APX RS2 fast digital camera 250 meters away from the explosion point. The velocities of the shock waves, blast wind and shrapnel fragments were calculated by using the distance they traveled on the images, the time elapsed in the recording and the frame numbers. Inferences were made about the injury profiles of the mannequins by examining their behavior during the explosion, their damage after the explosion and the number of shrapnel entry holes.

3. Material and Methods

Under this section, information about imagery, experimental methods used for blast loads calculations, image processing methods and blasting loads is given.

3.1. Blast Load Parameter Calculations

Understanding scaled distance requires an understanding of the scaling laws. In physics, the relationship between quantities that scale with each other is described by scaling laws. Force is usually scaled in relation to area or volume. The pressure factor used to calculate blast loads is a measure of the forces resulting from the blast [14]. Therefore, blast pressure effects at different distances can be estimated using scaled distance.

The effects of an explosive charge at a scaled distance are scaled with distance. The scaled distance is denoted by the letter 'Z'. In the calculated explosive charge graphs, the scaled distance refers to the horizontal plane. Scaled distance is one of the primary methods that should be used to calculate blast load parameters. There are 2 types of scaling methods, Hopkinson- Cranz and Sachs.

The Hopkinson Cranz scaling method uses the distance to the blast point and the explosive weight for

the scaled distance. It is also known as the cube root scaling law. Hopkinson-Cranz method is the most preferred method for calculating the scaled distance. Equation 1 shows the Hopkinson-Cranz scaling law.

$$Z = \frac{R}{\sqrt[3]{W}} \quad (1)$$

In Equation 1, Z represents the scaled distance, R represents the distance to the explosive material and W represents the weight of the explosive material.

The Sachs scaling method is used to calculate blast loads that occur at heights where atmospheric conditions can change. Ambient conditions are important for the blast wave. This is because the wave travels through the air. At high altitudes, atmospheric (air) pressure and air density decrease. There are many experimental formulas for the calculation of blast loads in the literature. The Kingery-Bulmash method is the most widely accepted method in the field of engineering and is commonly used by military units. Kingery-Bulmash used polynomial formulations derived from experiments for both spherical and hemispherical blast wave calculations. The equations are derived from data obtained from explosive tests using explosive weights ranging from 1 kg to 40,000 kg. For hemispherical blast waves, Z=0.05 $m/\sqrt[3]{kg}$ can be applied up to a scaled distance. Equation 2 and equation 2 give the general polynomial form of the Kingery-Bulmash method [14].

$$U = K_0 + K_1 * T \quad (1)$$

$$Y = C_0 + C_1U + C_2U^2 + C_3U^3 + \cdots + C_nU^n \quad (2)$$

In Equations 1 and 2, Y denotes the blast wave parameters, C_0, C_1, C_2, ... C_n, and K_0, K_1 are the constants. In Table 1 the constant values are given and an example formula calculation is shown. The formula calculates the incident pressure.

Table 1. Kingery-Bulmash Constants

Constants for U	K_0	K_1
	-0.21436278	1.3503424
Constants for Y=ip $i_p=C_0+C_1U+C_2U^2+C_3U^3+\ldots+C_8U^8$ $i_p*=10^{ip}$	C_0	C_1
	2.7807691	- 1.695898
	C_2	C_3
	0.15415937	0.51406073
	C_4	C_5
	0.098853436	0.026811234
	C_6	C_7
	0.10909749	0.0016284675
	C_7	C_8
	0.021463103	0.000145672

In Table 2 the constant values are given and an example scaled distance range is shown. The formula calculates the event pulse.

Table 2. Scaled distance and constants for event pulse

Constants for U (0.6<Z<0.9)	K_0	K_1
	2.0676190	3.076032
Constants for Y=i_s (0.6<Z<0.9)	C_0	C_1
	2.5245562	- 0.50299276
	C_2	C_3
	0.17133564	0.045017696

Table 3 shows the constants used to calculate the reflected pressure.

Table 3. Calculation constants for reflected pressure

Constants for U	K_0	K_1
	-0.24065732	1.3663771
Constants for Y=P_r	C_0	C_1
	3.4028321	- 2.2103087
	C_2	C_3
	-0.21853658	0.89531958
	C_4	C_5
	0.2498900	- 0.56924943
	C_6	C_7
	0.1179168	0.22413116

Using the Kingery-Bulmash method, a table of constants can be derived for each explosive charge parameter. The method is still accepted and used today because it provides high accuracy for both spherical and hemispherical waves. All parameters of this method are used to calculate the positive phase charges. The method is not used for negative phase parameters.

3.2. Image data

Explosion images were obtained by performing a controlled explosion in an isolated area. For this purpose, a high-speed camera, the Sony RX 10-4 (1,000 FPS) model, was used. This camera is resistant to dust and moisture and has a fast-focusing feature. The technical information about the camera is given in Table 4.

Table 4. Technical information about the camera

Info	Value
Pixel	20,1
Maximum resolution	5472 x 3648
Aspect ratio	1:1, 3:2, 4:3, 16:9
Sensor type	CMOS
Sensor size	1

The experimental setup designed for the explosion event is shown in Figure 1.

Figure 1. Experimental setup

The experimental setup in Figure 1 shows that the explosion test was performed in an isolated field. Necessary precautions were taken at the time of the explosion and no living being was harmed. In the experimental setup, explosives were placed on the concrete previously placed in the explosive field and a surface explosion was carried out. Figure 2 shows an image of the moment of explosion.

Figure 2. Image of the moment of explosion

The image shown in Figure 2 is one of the images that appeared at the moment of the explosion. As can be seen from the image, the resulting blast wave is not visible to the human eye. For this reason, various image processing techniques were employed, and the image of the blast wave was obtained.

The Sony RX 10-4 camera was positioned 250 meters away from the blast point. Explosion images were obtained with the camera at normal speed. The explosive was placed on concrete slabs to avoid a crater at the blast point. It was thought that the crater would distort the form of the blast wave. TNG was used as explosive material. TNG is similar to TNT in terms of its chemical structure but has a higher energy density. In order to determine the wave more clearly, the type of explosive with higher energy density, in terms of explosives close to TNT, was chosen.

3.3. Image processing techniques

Image processing is generally used to clear noise on images, make image improvements, sharpen images, and obtain meaningful information as a result of image analysis. Nowadays, it is used in many areas including health [9, 15], security [16-17], traffic control [18-19], agriculture [20-21], robotics [22-23], civil engineering [24], agricultural [25-26], etc.

Image processing is generally used to clear noise on images, make image improvements, sharpen images, or obtain meaningful data as a result of analyzing images [15, 27-28]. It takes place in four stages and these stages are given in Figure 3.

Figure 3. Image processing processes

Images used according to the purpose are collected during the image acquisition phase. Direct processing of the collected images may be ineffective in obtaining sufficient information, which is why the pre-processing stage is needed [29]. Furthermore, it is important to choose the right parameters [30].

At this stage, scaling, transitions in color space, noise removal, histogram operations, filtering, and morphological operations are applied. In the third stage, thresholding, labelling, edge extraction, and segmentation are performed. In the last stage, the process is completed by finding meaningful data from the image.

In this study, four different image processing methods were employed to detect the blast wave, with color transformation being the most significant among them. Through this process, the colored pixels of the explosion image were altered. Following color transformation, Fourier transform was employed to discern the image components in the frequency domain. Subsequently, conservative smoothing was implemented to reduce the intricacies within the explosion image. Finally, subtraction was carried out to calculate the disparity in pixel values between the two consecutive images. Figure 4 shows the steps of the image processing stage.

These approaches were specifically selected to effectively detect the blast wave in the image data. The color transform was used to highlight critical features of the blast, facilitating the identification of the key elements of the blast. The Fourier transform allowed the analysis of frequency components, which are essential for understanding the key patterns in the image. Conservative smoothing was applied to simplify the image by reducing noise, thus facilitating the detection of significant changes. Subtraction was then used to identify changes between successive images, important for capturing the dynamics of the blast wave.

The methods used are well established in the field of image processing and have been successfully applied in various studies to improve the detection and analysis of complex phenomena such as blast waves. This approach not only provides sensitive detection, but also contributes to the growing literature on the application of image processing techniques in the analysis of dynamic phenomena.

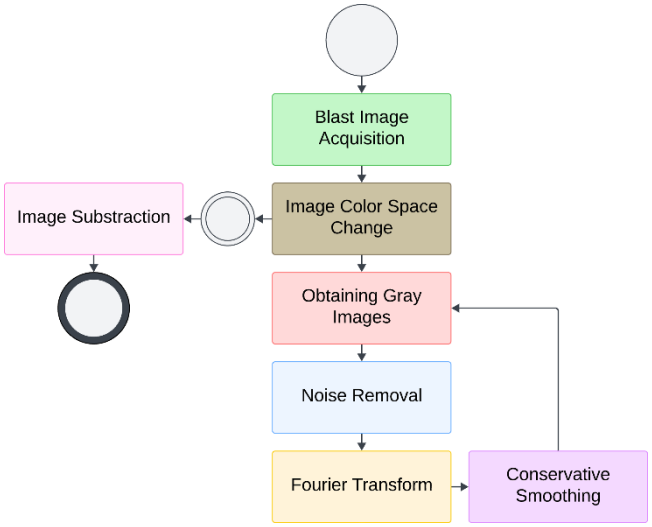

Figure 4. Flow chart of image processing methods applied to determine the blast wave

When the flowchart is examined, after the explosion video was obtained, the image was divided into frames. First, a color space transformation was performed on two consecutive frames (BGR RGB). Then the input images were converted into gray level images. As the second step, noise removal operations were performed on the input images. For this process, a Fourier transform was first performed on the input image and then conservative smoothing was applied. The reason for performing the process in this order is primarily to preserve the image quality and to protect the input image from high frequency components. The same process was then applied to the second image. First, color space transformation was performed on the two images. The images were converted to RGB model and the differencing process was performed. The application was completed by detecting the blast wave on the image.

The blast wave image obtained by image processing was analyzed using the Kingery-Bulmash method, which is the most accepted experimental method in the literature [31-32] and compared with the values obtained from experimental data. To compute the blast loads, the image containing the detected wave was initially considered. The distance covered by the blast wave along the ground surface was then measured. This process involved determining the distance using the Manhattan distance metric. The Manhattan distance is the sum of the total differences between two points on the vertical and horizontal axes of the matrix [33-34]. Image processing often involves grid layouts between pixels, and the Manhattan distance matches these layouts. The Manhattan distance only considers horizontal and vertical movements. For some applications, this can better model real-world distances, especially when movements occur only in these axes. The two endpoints of the wave identified on the output image were connected to calculate the length of the wave, thereby establishing the starting and ending regions of the detonation wave. Figure 5 shows the explosion wave image resulting from image processing.

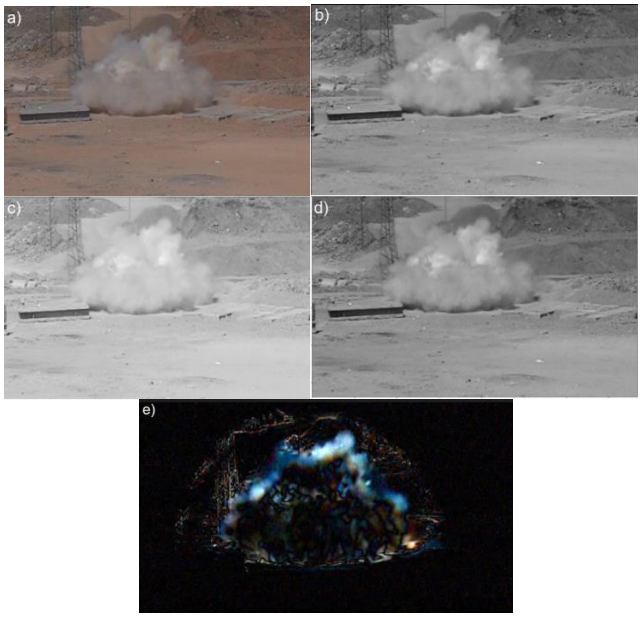

Figure 5. Steps of image processing and the resulting blast wave, a) Sample explosion image, b) Gray color image, c) Fourier transform applied image, d) Conservative smoothing applied image, e) Image subtraction

3.4. Blast loads

There are many experimental methods for calculating blast loads in the literature, but most of these methods are used in the analysis of spherical explosion waves [20]. Since surface explosion was performed in the study, the explosion wave form is hemispherical. For this reason, since the Kingery-Bulmash method uses a polynomial formula valid for hemispherical blast waves, this method was chosen in the analysis step and the loads of the blast were calculated. The Kingery-Bulmash method is the most accepted method in the field of engineering and commonly used by military units [35-36]. The formula generated was derived from data collected across a range of explosive weights, spanning from 1 kg to 40,000 kg. Explosion loads are composed of several parameters, as outlined in Table 5.

Table 5. Blast load parameters

Parameter	Explanation
Arrival time (s)	Time for the blast wave to reach peak pressure
Incident pressure (kPa)	Pressure corresponding to the blast wave
Reflected pressure (kPa)	The pressure of the reflected wave that returns after the incoming blast wave hits the surface
Reflected impact (kPa-ms)	The impact of the reflected wave
Event impact (kPa-ms)	Impact effect corresponding to the blast wave
Shock front velocity (m/s)	Velocity of the blast wave at the shock front
Weight (kg)	Weight of explosive material
Distance (m)	Distance to explosive material

There are two more important parameters that need to be taken into consideration when calculating blast loads, apart from experimental methods [37-38]. These; TNT is the unit of equivalent weight and scaling laws. Since there are many explosives of different types and structures, a common unit must be used to calculate blast loads. For this reason, TNT Relative Effect Factor (REF) is preferred in experimental studies. TNT explosive type has been standardized as the type of explosive widely used in many test explosions and explosion experiments, and its explosion charge characteristics are similar to the charge characteristics of most explosives [7]. TNT equivalent weight is calculated when an explosive type other than TNT will be used.

Scaling laws are used to show the relationship between distance and pressure. At scaled distance, the effects of an explosive charge scale with distance. Scaled distance is indicated by the *Z*. In the calculated explosive load graphs, the scaled distance refers to the horizontal plane. There are two different scaling laws including Hopkinson-Cranz and Sachs. Hopkinson-Cranz scaling law states that the effects and parameters of two different explosives with the same dimensions at the same distances are the same, provided that the ambient conditions are the same for both. It is also known as the cube root scaling law. On the other hand, Sachs scaling law is a scaling method used in calculating blast loads occurring at altitude where atmospheric conditions [39] may change.

In this study, TNG (Trinitroglycerin) explosive was used as the explosive type. In the selection of explosives, the type of explosive that was most easily accessible and whose chemical structure was closest to TNT was chosen to be used in the experimental study. This is because the TNT equivalent weight is close due to this chemical structure. The TNT REF value of the TNG explosive was found to be approximately '1.23' and is shown in Table 6. As a result of the study, existing methods were reviewed and the importance of explosive location and explosive waveform in the selection of methods for the calculation of blast load parameters was emphasized.

Table 6. TNG REF value

Parameter	TNG (Trinitroglycerin)	TNT (Trinitrotoluene)	Ratio
Detonation Velocity (m/s)	7700	6900	≈1.12
Energy Content (MJ/kg)	6.3	4.7	≈1.34
Average REF Value	≈1.23		

To calculate blast load parameters, first, it is necessary to determine the weather conditions in which the explosion will occur or have occurred. If the air is atmospheric, Sachs scaling law should be used, if it is not atmospheric, Hopkinson-Cranz scaling law should be used. The type of explosive used or will be used later must be known. Accordingly, the TNT equivalent weight should be calculated. To determine the effects of the explosive and the form of the blast wave, it must be selected whether the explosion is free air, air or surface explosion. Then, the methods for calculating the blast load parameters must be decided. Once the method is determined, explosion load parameters can be calculated.

As can be seen from these explanations, there are various steps involved in determining the blast loads of a particular explosion. All these steps take time and require processing load. In order to avoid these limits, in this study, the wave of the explosive was determined using image processing methods and the blast n loads were estimated from the shock wave images. A visual summary showing all these processes of the study is given in the flow chart in Figure 6.

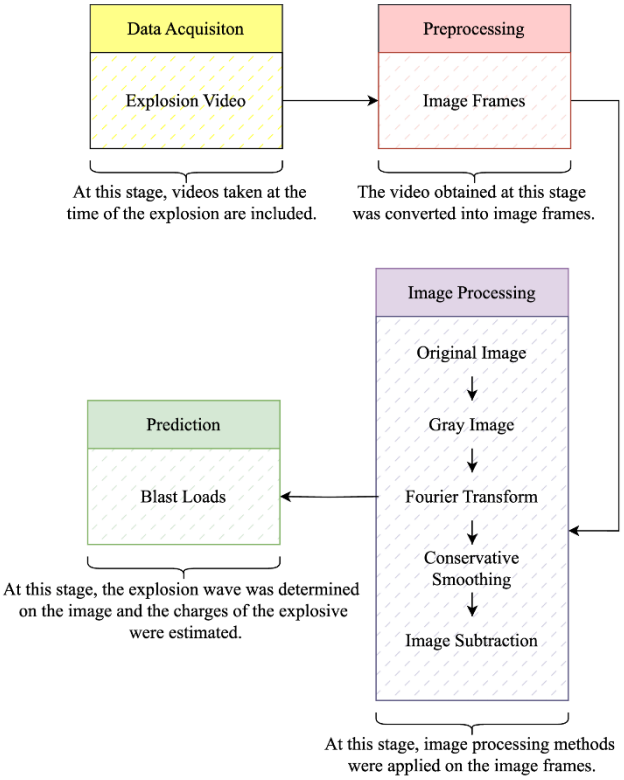

Figure 6. Flow chart of the study

4. Application Results and Discussion

The main purpose of the study is to predict blast loads from the image of the blast wave. In traditional approaches, empirical formulas are used to determine the loads of a blast, but these formulas are more effective in areas where controlled explosions are carried out. In places where uncontrolled explosions occur, the use of these formulas takes time and requires a large number of analysis procedures. However, with the application developed in this study, blast loads could be determined from only one image. The explosion wave is difficult to see with the naked eye, so the waveform was obtained using image processing methods. The resulting waveform is shown in Figure 7.

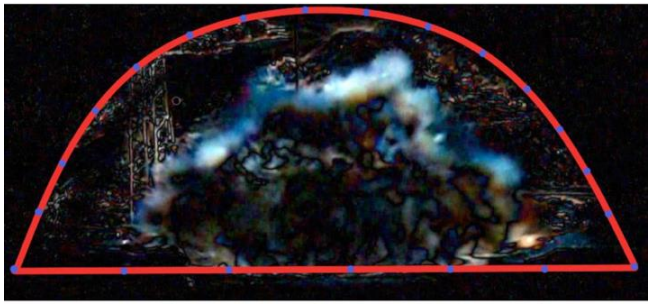

Figure 7. The explosion wave determined at the end of the image processing process

An application has been developed that takes the Manhattan distance as a parameter on the image from which the waveform is obtained. Accordingly, the application calculates the horizontal length of the blast wave using the Manhattan distance method, makes unit conversions and calculates it in meters. The distance of the blast wave is given in Figure 8.

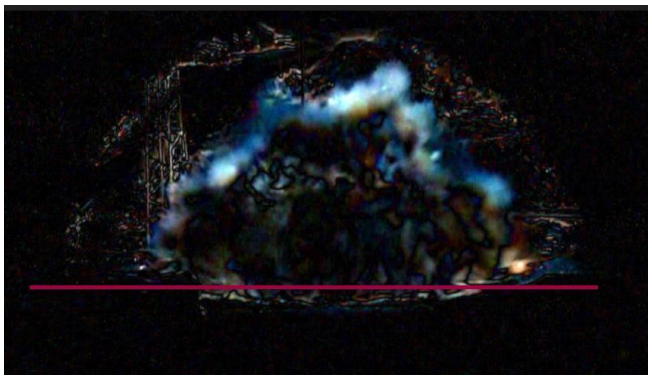

Figure 8. Distance of a blast wave

The value of the distance given in Figure 7 was initially calculated as 1,102 inches by using the Manhattan Distance method in combination with pixel measurements. To obtain the real distance, the pixel measurements were scaled using a reference dimension, resulting in a real distance of 28 meters. After converting the distance to meters, the shock front velocity was calculated, and blast loads were predicted using the positive phase duration from the data generated by the Kingery-Bulmash method. In Table 7, the blast loads obtained as a result of the prediction process and the blast loads calculated with Kingery-Bulmash are compared.

Table 7. Predicted blast loads and calculated blast loads by the Kingery-Bulmash method

Parameter	Predicted	Calculated
Arrival time (s)	73.08	73.1
Incident pressure (kPa)	3.98	3.92
Reflected pressure (kPa)	8.11	7.97
Reflected impact (kPa-ms)	20.44	20.17
Event impact (kPa-ms)	11.53	11.39
Shock front velocity (m/s)	345.90	345.83
Weight (kg)	1	1
Distance (m)	28	28

When the results given in Table 7 are examined, it is seen that the values of the calculated data and the predicted data (arrival time, incident pressure, reflected pressure, reflected impact, event impact, shock front velocity, weight, distance) are quite close. Using the distance-velocity relationship of the image of the blast wave taken after the explosion, the time since the beginning of the explosion was determined and the explosive weight was decided. Other blast loads were correlated with the shock front velocity value and calculated. In steps calculated with Kingery-Bulmash, the distance of a 1 kg explosive is 28 m. Since the distance calculated as a result of image processing was 28 m, in the data set created with Kingery-Bulmash, the part where the distance was 28 m was selected and the blast loads of this part were compared. According to the experimental formula, the arrival time of a 1kg explosive was calculated as 73.1 s, but as a result of the analysis made with image processing, this result was predicted as 73.08 s. While the incident pressure was predicted as 3.98 kPa, the actual value was calculated as 3.92 kPa. The reflected pressure, as determined through image processing, was predicted at 8.11 kPa, while the reflected pressure was predicted at 20.44 kPa/ms. However, upon examination of the actual data, the reflected pressure was found to be 7.97 kPa, and the reflected pulse was computed to be 20.17 kPa/ms. The event impact and shock front velocity loads were nearly identical in their predicted values. Through the prediction process, the event impact was determined as 11.53 kPa/ms, whereas the Kingery-Bulmash method yielded a slightly lower calculation of 11.39 kPa/ms for this rate. The shock front velocity determined by the Kingery-Bulmash method was 345.83 m/s. Through the prediction process, the calculated shock front velocity closely matched the actual value at 345.90 m/s.

In order to clearly demonstrate the performance of the method, the relative error was calculated. Relative error provides a scale-independent comparison of the error to the true value. This helps to understand the difference in error between small and large values when evaluating model performance [40]. The relative error results are given in Table 8.

Table 8. Relative error values calculated for each blast load

Parameter	Error Rate
Arrival time (s)	0.0274
Incident pressure (kPa)	1.51
Reflected pressure (kPa)	1.73
Reflected impact (kPa-ms)	1.32
Event impact (kPa-ms)	1.21
Shock front velocity (m/s)	0.0202

Upon reviewing the findings presented in Table 8, it becomes evident that the predicted data closely aligns with the results obtained from the experimental study, displaying a high degree of similarity. The reflected pressure exhibited the highest error value, whereas the error was minimal for the shock front velocity. In critical systems such as healthcare, aviation, automotive safety, and nuclear energy management, it is crucial to minimize error margins, often aiming for values approaching zero. Overall, none of the error percentages surpassed 2%,

underscoring the effectiveness of the image processing procedure.

It has been observed that the calculated data have almost the same values as the data recorded from the experimental data. Since the weight information of the explosive was not entered into the application, the weight of the explosive was also calculated and found to be the same as the weight used in the explosion. A TNG type explosive weighing 1 kg was used in the explosion, and application estimates ultimately estimated the weight of the explosive as 1 kg. Figure 9 and Figure 10 show the graphs of the blast loads calculated and predicted by the Kingery-Bulmash method, respectively.

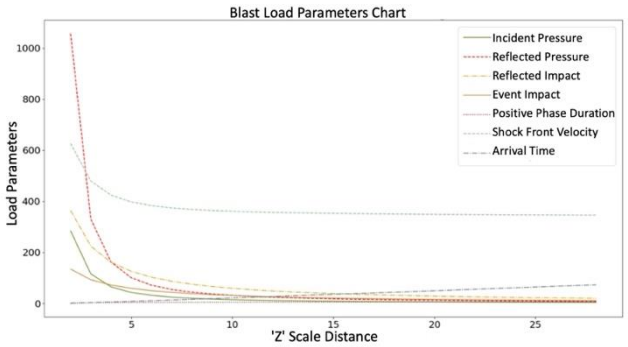

Figure 9. Blast loads chart calculated with Kingery-Bulmash

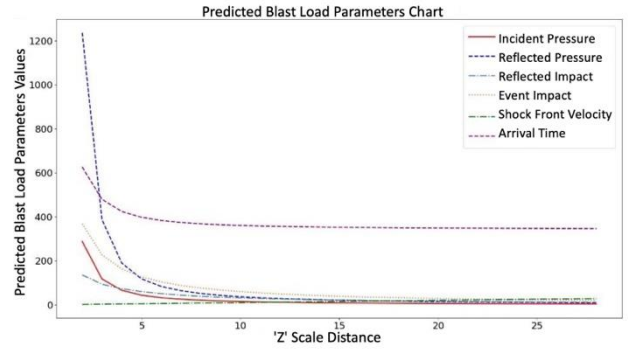

Figure 10. Blast loads chart predicted by the proposed model

When the given graphs are compared and examined, it is seen that the obtained values almost completely coincide with the data obtained from the calculated data.

Although effective results were obtained in this study, the study has several limitations. These can be expressed as follows:

- It is more suitable to use high-speed, slow-motion cameras to detect the wave image, so that the wave can be obtained by image processing methods.
- A wider database can be obtained by controlled detonation of explosives of different weights. With the image data obtained, sufficient test data can be created for artificial intelligence methods. It is a known fact that as the number of data increases, the prediction accuracy becomes more reliable, regardless of the study [41].
- By adding measurement sensors to the explosion area, realistic calculated data can be obtained for analysis and prediction of wave effect.
- Using thermal cameras, the area where the explosion occurred, and the explosion waveform can be predicted.

5. Conclusion

In this study, blast loads were predicted from the blast wave by using image processing techniques and the results were compared with the data obtained with experimental formula. The study consisted of four stages. In the first stage, a video recording of the explosion was made. In the second stage, images were obtained from videos and converted to the image frames. In the third stage, various image processing methods were applied on the images obtained and a blast wave form was determined. In the last stage, explosion loads were predicted based on the blast wave form. The study's analysis unequivocally demonstrates the considerable value of employing image processing for predicting blast loads. The effective utilization of diverse image processing techniques and computer vision algorithms not only highlights the promise of this approach but also signifies the possibility of exploring novel avenues for future research and applications. To conclude, the results of this study underscore the efficacy of image processing for predicting blast loads, showcasing its potential influence across multiple domains including safety, structural engineering, and disaster management. Future research endeavors focusing on refining and advancing these methodologies will undoubtedly enhance predictive technologies and safety protocols in contexts involving blast loads.

Very low error rates (0.0274% and 0.0202%) were obtained for arrival time and shock front velocity. This shows that the method is very successful in estimating these two parameters. The error rates for incident pressure, reflected pressure, reflected impact and event impact ranged between 1.21% and 1.73%. This shows that the predicted values are quite close to the calculated values, but the model is not perfect in these parameters. Further improvements can be made in these parameters. TNG explosives of different weights were detonated in the air and on the surface, and images were taken and stored with a high-speed camera for use in this study and future studies.

Author contributions

Dilan Onat Alakuş: Data Acquisition, Analysis, Data Calculation, Writing, Visualization, Field Work.
İbrahim Türkoğlu: Conceptualization, Reviewing and Editing.

Conflicts of interest

The authors declare no conflicts of interest.

References

1. Jankůj, V., Mynarz, M., & Lepík, P. (2022). Uncontrolled and Controlled Destruction of Acetylene Pressure Cylinders. *Applied Sciences*, *12*(7), 3577. https://doi.org/10.3390/app12073577
2. Sun, K., & Zhang, Q. (2021). Experimental study of the explosion characteristics of isopropyl nitrate aerosol under high-temperature ignition source. Journal of Hazardous Materials, 415, 125634. https://doi.org/10.1016/j.jhazmat.2021.125634
3. Moore, P. E. (1996). Suppressants for the control of industrial explosions. Journal of Loss Prevention in the Process Industries, 9(1), 119–123. https://doi.org/10.1016/0950-4230(95)00045-3
4. Mckenzie, G., Samali, B., & Zhang, C. (2019). Design criteria essential for an uncontrolled demolition (explosion). Asian Journal of Civil Engineering, 20, 1-19. https://doi.org/10.1007/s42107-018-00110-0
5. Dobashi, R., Kawamura, S., Kuwana, K., & Nakayama, Y. (2011). Consequence analysis of blast wave from accidental gas explosions. Proceedings of the Combustion Institute, 33(2), 2295-2301. https://doi.org/10.1016/j.proci.2010.07.059
6. Sommersel, O. K., Bjerketvedt, D., Christensen, S. O., Krest, O., & Vaagsaether, K. (2008). Application of background oriented schlieren for quantitative measurements of shock waves from explosions. Shock Waves, 18, 291–297. https://doi.org/10.1007/s00193-008-0142-1
7. Mizukaki, T., Wakabayashi, K., Matsumura, T., & Nakayama, K. (2014). Background-oriented schlieren with natural background for quantitative visualization of open-air explosions. Shock Waves, 24, 69–78. https://doi.org/10.1007/s00193-013-0465-4
8. Li, G., Agir, M. B., Kontis, K., Ukai, T., & Sriram, R. (2019). Image processing techniques for shock wave detection and tracking in high-speed schlieren and shadowgraph systems. Journal of Physics: Conference Series, 1215(1), 012021. https://doi.org/10.1088/1742-6596/1215/1/012021
9. Chhabra, C., & Sharma, M. (2021). Machine learning, deep learning and image processing for healthcare: A crux for detection and prediction of disease. Proceedings of Data Analytics and Management, 305–325. Springer. https://doi.org/10.1007/978-981-16-6285-0_25
10. Silay, R., & Karacı, A. (2021). Patlayıcı Etki Analizi Simülasyon Yazılımının Geliştirilmesi ve Basınç Dalgası Parametrelerinin Derin Öğrenme ile Tahmin Edilmesi. Duzce University Journal of Science and Technology, 9(6), 303-315. https://doi.org/10.29130/dubited.1014063
11. [11] Yang, H., Du, L., & Mohammadi, J. (2021). A shock wave diagram based deep learning model for early alerting an upcoming public event. Transportation Research Part C: Emerging Technologies, 122, 102862. https://doi.org/10.1016/j.trc.2020.102862
12. Mohr, L., Benauer, R., Leitl, P., & Fraundorfer, F. (2019). Damage estimation of explosions in urban environments by simulation. ISPRS - International Archives of the Photogrammetry, Remote Sensing and Spatial Information Sciences, XLII-3/W8, 253–260. https://doi.org/10.5194/isprs-archives-XLII-3-W8-253-2019
13. Özer, M. T., Coşkun, K., Öğünç, G. İ., Eryılmaz, M., Yiğit, T., Kozak, O., Apaydın, K., & Uzar, A. İ. (2010). The disguised face of blast injuries: Shock waves. Ulus Travma Acil Cerrahi Derg, 16(5), 395–400. https://tjtes.org/jvi.aspx?pdir=travma&plng=eng&un=UTD-93695
14. Onat Alakuş, D. Patlama enerjisinin görüntü işleme ile etkisinin analizi (Yüksek lisans tezi, Fırat Üniversitesi, Fen Bilimleri Enstitüsü, Elazığ, Türkiye). YÖK Tez Merkezi. https://tez.yok.gov.tr/UlusalTezMerkezi
15. Al-khafajı, Y. S. A., K. Muallah, S., & R. Ibraheem, M. (2018). Detection of Eczema DISEASE by using Image Processing. The Eurasia Proceedings of Science Technology Engineering and Mathematics (2), 273-287. http://www.epstem.net/en/pub/issue/38904/455955
16. Kumar, R., & Joshi, K. (2020). Enhancing network security for image steganography by splitting graphical matrix. International Journal of Information Security Science, 9(1), 13-23 https://dergipark.org.tr/en/pub/ijiss/issue/67165/1048731
17. Eylence, M., Yücel, M., Özmen, M.M., & Aksoy, B. (2022). Railway security system design by image processing and deep learning unmanned aerial vehicle. Turkish Journal of Nature and Science, 11(3), 150-154 https://doi.org/10.46810/tdfd.1112957
18. Arslan, B., Büyükkaya, T., & Alparslan Ilgın, H. (2016). Real-time traffic sign detection and recognition. Communications Faculty of Sciences University of Ankara Series A2-A3 Physical Sciences and Engineering, 58(2), 70–83. https://doi.org/10.1501/commua1-2_0000000097
19. Pamuk, N. (2022). Vehicle Plate Recognition System Using Image Processing. The Eurasia Proceedings of Science Technology Engineering and Mathematics, 21, 328-334. https://doi.org/10.55549/epstem.1226649
20. Erkan, Y. R., & Kahramanlı Örnek, H. (2019). Mushroom species detection using image processing techniques. International Journal of Engineering and Innovative Research, 1(2), 71–83. https://dergipark.org.tr/en/pub/ijeir/issue/50628/597807
21. Karadöl, H., Kuzu, H., & Keten, M. (2023). Estimation of Soybean Seeds Weight Using Image Processing. Black Sea Journal of Agriculture, 6(5), 511-515. https://doi.org/10.47115/bsagriculture.1324253
22. Hyder, U., & Talpur, M. R. H. (2024). Detection of cotton leaf disease with machine learning model. Turkish Journal of Engineering, 8(2), 380-393. https://doi.org/10.31127/tuje.1406755
23. Hamida El Naser, Y., Karayel, D., Demirsoy, M. S., Sarıkaya, M. S., vd. (2024). Robotic Arm Trajectory Tracking Using Image Processing and Kinematic Equations. Black Sea Journal of Engineering and Science, 7(3), 436-444. https://doi.org/10.34248/bsengineering.1445455

24. Aydın, M., & Kurnaz, T. F. (2023). An alternative method for the particle size distribution: Image processing. Turkish Journal of Engineering, 7(2), 108-115. https://doi.org/10.31127/tuje.1053462
25. Meghraoui, K., Sebari, I., Bensiali, S., & Kadi, K. A. (2022). On behalf of an intelligent approach based on 3D CNN and multimodal remote sensing data for precise crop yield estimation: Case study of wheat in Morocco. Advanced Engineering Science, 2, 118-126. https://publish.mersin.edu.tr/index.php/ades/article/view/329
26. Pajaziti, A., Basholli, F., & Zhaveli, Y. (2023). Identification and classification of fruits through robotic system by using artificial intelligence. Engineering Applications, 2(2), 154-163. https://publish.mersin.edu.tr/index.php/enap/article/view/974
27. Kuncan, F., Öztürk, S., & Keleş, F. (2022). Image processing-based realization of servo motor control on a Cartesian Robot with Rexroth PLC. Turkish Journal of Engineering, 6(4), 320-326. https://doi.org/10.31127/tuje.1004169
28. Boopathi, S., Pandey, B., & Pandey, D. (2023). Advances in artificial intelligence for image processing: Techniques, applications, and optimization. In Advances in Artificial Intelligence for Image Processing: Techniques, Applications, and Optimization (pp. 73–95). IGI Global. https://doi.org/10.4018/978-1-6684-8618-4.ch006
29. Gordani, O., & Simoni, A., (2024). Leveraging SVD for efficient image compression and robust digital watermarking. Advanced Engineering Science, 4, 103–112. https://publish.mersin.edu.tr/index.php/ades/article/view/1496
30. Demiröz, A., Barstugan, M., Saran, O., & Battal, H. (2023). Determination of compaction parameters by image analysis technique. Advanced Engineering Science, 3, 137-150. https://publish.mersin.edu.tr/index.php/ades/article/view/1192
31. Bueno, J.R., Leger, P., Loriggio, D.D., & Sousa, A.C. (2021). Blast computer simulation: code for blast analysis using MatLab. Revista Sul-Americana de Engenharia Estrutural, 18, 44-49 https://doi.org/10.5335/rsaee.v18i1.8770
32. Jankura, R., Zvaková, Z., & Boroš, M. (2020). Analysis of mathematical relations for calculation of explosion wave overpressure. Proceedings of CBU in Natural Sciences and ICT, 1, 21–27. https://doi.org/10.12955/pns.v1.116
33. Veerashetty, S., & Patil, N. (2019). Manhattan distance-based histogram of oriented gradients for content-based medical image retrieval. International Journal of Computers and Applications, 43, 1–7. https://doi.org/10.1080/1206212X.2019.1653011
34. Gao, X., & Li, G. (2020). A KNN model based on Manhattan distance to identify the SNARE proteins. IEEE Access, 8, 112922–112931. https://doi.org/10.1109/ACCESS.2020.3003086
35. Tyagi, L., Kumar, V., & Chakraborty, S. (2020). Explosion consequence analysis for military targets through support vector machines. In Proceedings of the 2020 7th International Conference on Recent Trends in Information Technology (ICRITO) (pp. 948–951). https://doi.org/10.1109/ICRITO48877.2020.9197866
36. Viano, D. (2023). Injury and death to armored passenger-vehicle occupants and ground personnel from explosive shock waves. Scientific Reports, 13. https://doi.org/10.1038/s41598-023-29686-7
37. Dennis, A. A., Pannell, J. J., Smyl, D. J., & Rigby, S. E. (2021). Prediction of blast loading in an internal environment using artificial neural networks. International Journal of Protective Structures, 12(3), 287–314. https://doi.org/10.1177/2041419620970570
38. Shirbhate, P. A., & Goel, M. D. (2021). A critical review of blast wave parameters and approaches for blast load mitigation. Archives of Computational Methods in Engineering, 28(4), 1713–1730. https://doi.org/10.1007/s11831-020-09436-y
39. Singh, K., Gardoni, P., & Stochino, F. (2020). Probabilistic models for blast parameters and fragility estimates of steel columns subject to blast loads. Engineering Structures, 222, 110944. https://doi.org/10.1016/j.engstruct.2020.110944
40. Mehdi, R., & Günal, A. Y. (2023). The impact of land use and slope change in flow coefficient estimation. Engineering Applications, 2(3), 254–264. https://publish.mersin.edu.tr/index.php/enap/article/view/1101
41. Zela, K., & Saliaj, L. (2023). Forecasting through neural networks: Bitcoin price prediction. Engineering Applications, 2(3), 218–224. https://publish.mersin.edu.tr/index.php/enap/article/view/874

© Author(s) 2024. This work is distributed under https://creativecommons.org/licenses/by-sa/4.0/